The 15th International Symposium on Magnetic Bearings, August 3-6, 2016, Mojiko Hotel, Kitakyushu, Japan

ISMB15

Design and commissioning of a 3.3 MW motor-driven compressor fully supported on active magnetic bearings

Richard JAYAWANT* and Andrea MASALA*

*Waukesha Magnetic Bearings, Unit K, Downlands Bus. Pk.,
Lyons Way, Worthing, W. Sussex, BN14 9LA, United Kingdom
E-mail: rjayawant@waukbearing.com

Abstract

This paper describes the design and commissioning of active magnetic bearings (AMBs) for a 3.3 MW motor-driven compressor. The total string comprises a motor coupled (via a flexible coupling) to a compressor, with the two machines mounted in separate casings. The design of the compressor AMBs, in particular the rotordynamic design, is described together with the commissioning experience for both the compressor and the coupled string. The use of third-generation Automated Commissioning tools in the initial setup and the dynamic tuning of the machine is described. These tools were deployed remotely and the impact of this remote mode of commissioning on the required work methods, including the impact of variable performance in Internet connectivity and the tools required for communication across large differences in time zones, is examined. Particular issues encountered during the commissioning, triggered by use of close clearance seals, are discussed; these include impact on the use of the Automated Commissioning tools, impact on the vibration performance of the machine (with solutions to overcome these problems), and impact of stiction in the seals on the rotordynamic measurements. The results of the vibration measurements and sensitivity function measurements for the tuned machine are presented.

Keywords : Active Magnetic Bearings, Motor Compressor, Seal Cross-Coupling, FAT, Automated Commissioning, Remote Commissioning, API 617, Compressor

1. Introduction

Motor compressors fully supported on active magnetic bearings (AMBs) have been in service since the mid-1990s. Research and development has tended to focus on integrated motor compressors where the compressor and motor share a common rotor and a common casing (e.g., Vannini, et al., 2011 and Al-Aidarous and Shultz, 2014). There is, however, significant industry activity in the design and development of AMB-supported motor compressors with separate motor and compressor bodies where the machines are coupled via a flexible coupling (e.g., Groot, et al., 2000). The use of separate motor and compressor bodies allows high system flexibility, including independent choice of the motor and compressor vendors and easy customization of compressor performance curves to match required process conditions.

This paper presents experience gained during the design and OEM factory commissioning of an AMB system supporting a 3.3 MW motor-driven compressor. The motor and compressor were supplied by different vendors with a common AMB vendor. The integration of the overall machine was under the control of the compressor vendor. The completed equipment is destined for service in a natural gas booster station.

The compressor is a multi-stage machine and operates above the first free-free mode of the compressor. The resulting rotordynamic challenges are described together with the design approach used to achieve acceptable performance.

The commissioning of the system was conducted using third-generation commissioning tools, also known as Automated Commissioning tools. The results from the commissioning and a comparison of those results to the theoretical modelling conducted during the design phase of the project will be reviewed.

2. Design of the compressor and bearings

The AMB-equipped compressor is a 3.3 MW barrel-type centrifugal compressor for hydrocarbon gas boosting service covering a large operating range, with design suction pressure of 38.5 bar-g and discharge pressure of 79 bar-g. The operating speed of the compressor ranges between the minimum operating speed (MOS) of 6200 rpm and the maximum continuous speed (MCS) of 9400 rpm. The compressor bundle includes five impellers and a balance drum located at the drive end (DE) of the machine. Requirements for high thermodynamic efficiency of the compressor set a demand for tight radial clearances on impellers and balance drum seals. Abradable labyrinth seals with minimum radial clearance of 0.23 mm on impellers and on the balance drum were adopted by the compressor OEM.

Such seal clearances, comparable to the 0.2 mm nominal radial clearances of the auxiliary bearings, set a requirement for fine alignment processes and tolerances of the compressor bundle and auxiliary bearings to guarantee a minimum residual gap between the rotor and stator part of the machine and prevent heavy rubbing of the rotor seals during rotation or in case of rotor landing on auxiliary bearings during testing or machine operation.

The tight radial clearances also result in predicted dynamic cross-coupling and destabilizing effects on the rotor during operation at high speed and high compression ratio.

The AMB actuator consists of two radial active magnetic bearings and an axial, double-acting magnetic bearing located inboard at the non-drive end (NDE) of the compressor. There are five control axes: four radial and one axial. A summary of the main AMB characteristics are provided in Table 1. The AMB system also includes combined radial and axial inductive position sensors and a set of auxiliary bearings located outboard of the position sensor.

Table 1 Summary of AMB characteristics.

Radial AMB type	Heteropolar
Radial AMB diameter	101.6 mm
Radial AMB active length	100 mm
Radial AMB magnetic airgap	0.7 mm
Radial AMB load capacity (per axis)	3200 N
Axial AMB type	E-Core
Axial AMB gap	0.7 mm
Axial AMB outer diameter	353 mm
Axial AMB load capacity (nominal)	42000 N

The selected auxiliary bearings are a hybrid design, combining proprietary rotor-mounted ball bearings and a bushing type stator to guarantee endurance under high radial and axial loads and extended coastdown times in case of an emergency landing event.

To meet the stringent requirements for Zone-1 Hazardous Area Protection set for the complete machine and to guarantee adequate cooling of the AMBs and auxiliary bearings, the AMB cavities were purged with clean, low-pressure inert gas. A minimum pressure of 50 Pa-g across the AMB cavity was required to meet the EEx-p requirements for the pressurized protection scheme. To this aim, a cooling gas inlet pressure of 0.2 bar-g and 50°C was fed into each AMB cavity. The low-pressure AMB cavities were separated from the high inlet suction pressure of the compressor by means of tandem dry gas seals (DGSs) located on each side of the compressor bundle.

A model of the AMB actuator hardware and a schematic of the rotor model are depicted in Fig. 1 and 2 respectively. The overall rotor length is 2225 mm, with a span of 1673 mm between the radial AMBs; the total rotor mass (including half the coupling weight) is 320 kg.

Although the AMB system used for this application is based on proven design and construction, specific challenges associated with the stability of the compressor were envisaged during the design phase due to the combination of stringent performance requirements set by ISO 14839-3 and API 617 7th Ed., the presence of a bending mode in the operating speed range, and the expected destabilizing seal effects.

Based on free-free mode shape analysis (Fig. 2), satisfactory critical damping of the 1st bending mode within the operating speed range was expected, due to good observability and controllability characteristics being predicted. Greater control challenges were expected for higher frequency modes; the close proximity of the deflected mode shape nodes to the NDE and DE actuator positions and uncertainty in the correct interlacing of the zero-poles would make proper damping and achievement of ISO 14839-3 sensitivity transfer function requirements in the entire 0-2 kHz frequency range challenging.

To verify the accuracy of the rotor modelling and reduce tuning time during machine commissioning, a ping test of the rotor in free-free configuration was performed by the OEM. The test results showed generally good matching between

predicted (calculated) and measured mode frequencies (Table 2) and mode shapes.

Table 2 Free-free test comparison.

Free-free modes	1st free-free bending	2nd free-free bending	3rd free-free bending	4th free-free bending
Calculated [Hz]	135.1	292.8	471.6	705.7
Measured [Hz]	135.9	299.5	477.6	638.8
Deviation [%]	0.60	2.29	1.27	-9.49

The critical speed ratio of the rotor (2.4) and average gas density (57 kg/m^3) when the compressor was operating at MCS and close to the surge limit, combined with the tight seals clearances, resulted in a predicted average destabilizing cross-coupling stiffness of 7E+05 N/m induced by the seals. The number of teeth and the pressure drop across the seal resulted in an even higher destabilizing cross-coupling stiffness of 2.8E+0.6 N/m and a direct negative stiffness of -1.3E+06 N/m on the balance drum. Uncertainty in the predictability of such destabilizing seals coefficients, as reported by Kocur, et al. (2007), was expected. To deal with aerodynamic-induced instability, a decentralized control architecture with dedicated and easily tunable low-frequency filter configurations was selected. A complete Level-2 analysis, according API 617 Standards, and extensive sensitivity analysis on seals coefficients were conducted.

The compressor was designed to be coupled to a high-speed motor powered by a variable speed drive and connected to the compressor by means of high-speed flexible coupling. A lateral rotordynamic analysis of the entire motor-compressor train was performed to confirm proper separation of the compressor and motor dynamics through the flexible coupling. To this aim, the 1400 kg electric motor rotor model was added to the compressor model and the two rotors were coupled by means of a flexible coupling model representing both inertial and stiffness properties of the coupling (Fig. 3). The effect of the electric motor on the compressor rotordynamics was evaluated in terms of eigenvalues, unbalance response and sensitivity analysis. The unbalance response results and the sensitivity transfer functions calculated for the compressor rotor and the full rotor train models (Fig. 4) revealed very good matching, confirming dynamic uncoupling between motor and compressor.

A Zephyr controller was selected for both the compressor and the motor AMBs. The controllers were packaged into a single control cabinet along with a fitted spare controller and associated power supplies and cable marshalling (Fig. 5). The fitted spare configuration allows for rapid changeover in the unlikely event of issues and removes the complex logistics associated with long-term storage of spare parts. Zephyr controllers are full-functionality, network-capable controllers that support Automated Commissioning tools. The specification for the controllers is provided in Table 3.

Table 3 AMB controller specification.

Amplifier DC link voltage	390 V
Magnet drive type	PWM switching amplifier
Peak magnet drive	28.5 A
Sensor type	Inductive sensor / 22.5KHz
Dimensions	90 x 33 x 50 cm (w x d x h)

3. Overview of commissioning setup, including Automated Commissioning tools

Prior to the commissioning of the compressor and full train, the motor was commissioned at the motor vendor's factory. At the start of compressor commissioning, the motor AMB controller was re-installed in the control cabinet and the motor installed on the test bed next to the compressor.

With the compressor OEM having installed the AMBs in the compressor and made connections between the control cabinet and machine, initial commissioning of the compressor was performed without the compressor coupled to the motor. The coupling hub was fitted but without the coupling spacer. This initial static levitation and calibration was conducted using Automated Commissioning tools.

Automated Commissioning tools automate many of the routine functions performed during AMB commissioning, such as verifying the integrity of the machine build, clearances and associated field cabling; sensor configuration and

calibration; configuration and tuning of amplifier servo loops; and configuration and tuning of position servo loops. The tools rely on the internal measurement capabilities of the AMB controller and a web services interface. The web services interface provides access to all AMB parameters and to the results of measurements and data acquisition performed by the controller. Available data includes instantaneous values of measured and control variables, filtered (DC and amplitude) values of measured and control variables, spectra of measured and control variables, transfer function measurements, high-speed time domain data, and order tracked data related to measured variables.

While these measurements can be accessed via a conventional web browser interface (via local or remote connection), the use of the web services interface allows for sophisticated programmatic access to the data (Fig. 6).

To allow secure VPN access via the Internet, the compressor OEM connected a router to the local AMB controller network. The initial phase of commissioning was conducted in two shifts, with a local AMB specialist handling the first shift and a specialist who had connected remotely handling the second shift.

Any connection via the Internet is not a robust connection and frequent loss of VPN connection was encountered during the commissioning. In Automated Commissioning, data transfer between the AMB controller and the remote PC is minimized due to the data reduction inherent in the on-board signal processing performed by the AMB controller. This means that loss of connection does not present a major problem; however, additional communication channels, such as text messaging or online chat, are desirable to facilitate efficient communication between the on-site engineer and the remote specialist. Automated Commissioning tools are fully detailed in Jayawant and Davies (2013, 2014).

Once the compressor was levitated on the AMBs, setup of the test stand was completed, including solo runs of the motor to verify inverter installation, alignment of the motor and compressor, fitting of the coupling spool (after which AMB-coupled machine tuning could proceed), and completion of the process loop.

4. Commissioning results and comparison with modelling

The centrifugal compressor underwent an extensive testing program at the OEM workshop before final acceptance from the end user. The test included the following steps:

a) AMB system commissioning
b) Load testing of the AMB to verify rated load
c) Mechanical running test
d) Compressor performance and full load test according to the ASME PTC-10 Type 2 test
e) Thermal test for Hazardous Area Certification
f) Full speed auxiliary bearing landing test

Steps (a) to (e) were all performed using a mixture of remote and on-site AMB specialists.

The AMB commissioning tasks included static levitation of the rotor and system identification (open loop transfer function and sensitivity transfer function measurement) to confirm controller parameters or a need for further tuning. To this aim, in addition to single axis transfer function measurements as specified by ISO 14839-3, a more conservative transfer function measurement based on in-phase and out-of-phase planar excitation of the rotor was performed. In these excitation methods, external disturbance is applied concurrently on each AMB, resulting in maximum excitation of the rotor bouncing or rocking modes. A comparison of sensitivity transfer functions with single axis, in-phase and out-of-phase excitation is provided in Fig. 7 and confirms the more conservative nature of the multi-axis excitation.

Although the rotor could be stably levitated with the original control parameters, the commissioning process verified that tight seal clearances and rotor stiction had detrimental effects on the rotor's stability during machine start-up. Changes in the dynamic characteristics of the system induced by contact with the seal could lead to system instability. To overcome this effect, changes to system gain during levitation were required. Contact between the rotor and seals was also demonstrated to negatively affect the accuracy of system identification measurements, particularly in the low frequency range and with the rotor at standstill. Transfer function measurements during low-speed rotation (500 rpm) were verified to be closer to the predicted low frequency response, due to reduced stiction effects from the labyrinth seals and increased clearances during and after rotor rotation.

A comparison of sensitivity transfer function measurements at standstill and at 500 rpm is presented in Fig. 8, along with the predicted sensitivity transfer function for the original un-tuned rotor model with final tuned AMB controller. Although the predicted natural frequencies were generally close to the measured system resonances, the predicted peak sensitivity transfer function magnitude was generally higher than the measured values, due to unavoidable deviations

between the rotor model and reality and conservative assumptions on rotor structural damping, assumed to be zero in the simulations.

Upon completion of system identification, only minor optimisation of the controller parameters was needed to correct deviations between predicted and measured rotor modes and to account for un-modelled housing dynamics.

Slight modification of the controller parameters to optimize the rotor response when running across the 1st bending mode, located within the operating speed range at 120 Hz, was also required. The final rotor response when the machine was running from standstill to MCS (Fig. 9) demonstrated good quality of rotor balancing and the capacity of the AMB to run the rotor through the 1st bending mode, inside the operating speed range, with low vibrations and dynamic currents even with no speed tracking filters applied.

Transfer function measurements on the compressor, when coupled or uncoupled from the motor, confirmed the separation of the compressor and motor dynamics, as predicted in the full-train rotordynamic analysis. However, tests conducted during ATEX certification testing with high unbalance levels (to excite full AMB load capacity) confirmed the possible transfer of dynamic loads from the motor to the compressor, and vice versa, through the flexible coupling when one of the machines is subject to high lateral vibrations.

Incidences of sub-synchronous excitation of the 1st rigid mode (20 Hz) of the compressor (Fig. 10) were identified when the machine operated under high load/high compression ratio condition, resulting from the increased destabilizing effects on impellers and balance drum labyrinth seals. Tighter than expected seals clearances, especially during operation, and differences between the test gas properties (N_2) and process gas mixture (hydrocarbons) were identified among the main drivers of the increased low frequency excitation level.

Low frequency (7 Hz and 14 Hz) aerodynamic excitation of the rotor originated from rotating stall on the compressor when operating at low flowrate condition.

Final adjustment of the AMB controller parameters to target higher stiffness and damping in the low frequency range reduced by nearly one order of magnitude the 1st rigid mode excitation driven by seal cross-coupling and the low frequency rotor vibration under rotating stall condition while preserving the high frequency stability performances of the system (Fig. 11).

5. Conclusions

The mechanical running test of the compressor confirmed proper matching between predicted and measured AMB system performance and rotordynamic performance. Seal-induced incidences of rotor response and aerodynamic static and dynamic excitation phenomena, partially predicted during the design phase, were experienced during the extensive testing program. Acceptable dynamic performance was achieved through optimisation of controller parameters. Detrimental effects on stability and measurement system accuracy resulting from stiction within the tight seals clearances were also addressed by the optimisation.

In all tests, the AMB system demonstrated good load capacity margins and good versatility for coping with different sources of excitation and changes in system dynamics. Improved predictability on compressor excitation phenomena, along with sensitivity analysis of system parameters, can improve overall system robustness.

Although API 617 7th Ed. was adopted at the beginning of the project, AMB system performances were generally verified against API 617 8th Ed. requirements. Overall, the analysis and test activity on the compressor confirmed robust performances and operation of the machine under API 617 8th Ed. and ISO 14839-3 requirements.

In line with the spirit of API 617 8th Ed., opportunities for gaining and sharing a common critical perspective between parties (AMB vendor, OEMs and end users) on machine and AMB system performance were identified:

- Simple and strict observance of API 617 and ISO 14839-3 standards should leave space for common understanding and trade-offs between different AMB system and machine performance indicators.
- Unconditional compliance to some legacy API 617 Standard requirements, such as unbalance response amplification factors, or demands for meeting Zone-A Peak Sensitivity Transfer function up to 2 kHz, as specified by ISO 14839-3, can result in unnecessary constraints during design or tuning processes.

Such requirements can be challenging to meet while maintaining robust vibration behavior when the machine is subject to unpredicted aerodynamic excitations.

Finally, the remote use of Automated Commissioning tools was shown to be an efficient and practical way of providing remote support to field commissioning, including the support of an extended work day through use of AMB

specialists in multiple time zones.

6. References

Al-Aidarous, M. and Shultz, R., Bearing System Reliability and Availability, Including Consideration of Magnetic Bearing Systems, Proceedings of the 3rd Middle East Maintenance and Reliability Conference, 2014,

Groot, W.H., Kummlee,H.,Lenderink, G.M., Shultz, R.R., Design and Experience with a 30,000 HP Magnetic Bearing Supported Motor Driven Turbocompressor for a Speed Range of 600 to ^300 RPM, Proceeding of the 29th Turbomachinery Symposium (2000), pp. 65-80.

Jayawant, R. and Davies, N., Integration of signal processing capability in an AMB controller to support remote and automated commissioning, Proceedings of the 1st Brazilian Workshop on Magnetic Bearings (2013), Available at http://www.magneticbearings.org/publications/

Jayawant, R. and Davies, N., Field experience with Automated Commissioning tools in both remote and local commissioning of active magnetic bearing systems," Proceedings of ISMB14 (2014), Available at http://www.magneticbearings.org/publications/

Kocur, J. A., Nicholas, J. C. and Lee, C. C., Surveying tilting pad journal bearing and gas labyrinth seal coefficients and their effect on rotor stability, Proceedings of the 36th Turbomachinery Symposium (2007), pp.1-10.

Vannini, G., Masala, A., Ortiz Neri, M., Evangelisti, S., Camatti, M., Svetti, F. and Bondi, S., Full load testing of a 12.5 MW vertical high speed subsea motor compressor, Proceeding of the 40th Turbomachinery Symposium (2011), pp. 79-92.

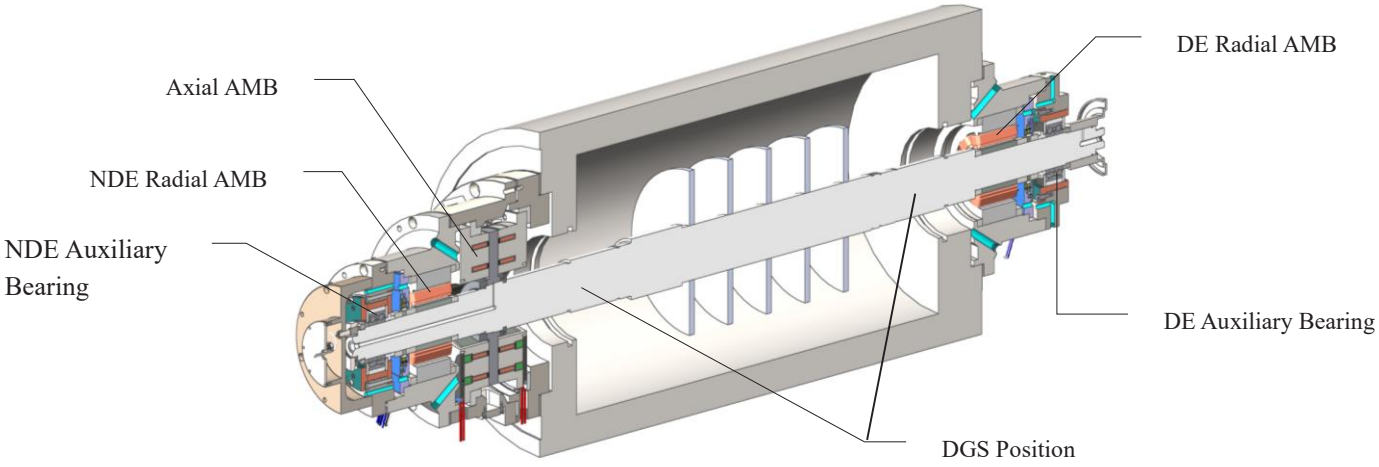

Fig. 1 AMB assembly on centrifugal compressor.

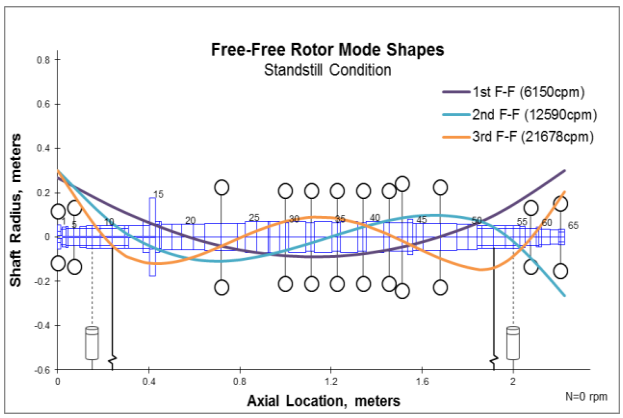

Fig. 2 Compressor rotor model with free-free mode shapes at standstill.

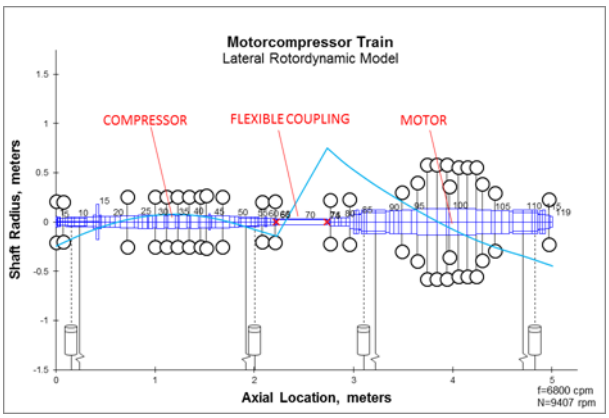

Fig. 3 Lateral rotordynamic model for full motor-compressor train.

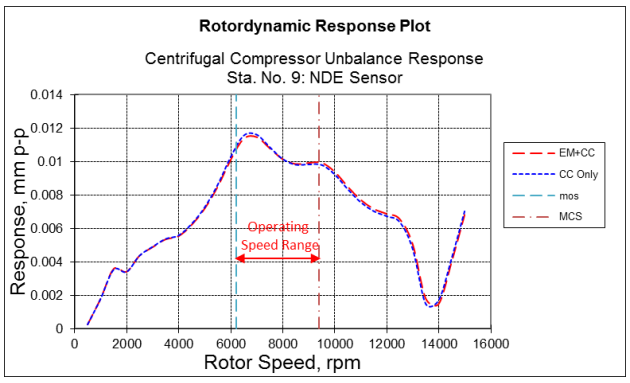

(a) NDE Unbalance Response – Case#3 NDE

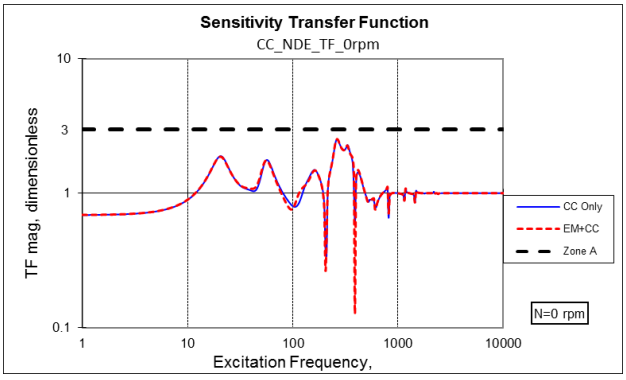

(b) NDE Sensitivity Transfer Function at 0 rpm

Fig. 4 Unbalance response and sensitivity transfer function analysis results for compressor only (CC) and compressor coupled to motor (EM+CC).

Fig. 5 AMB control cabinet during commissioning.

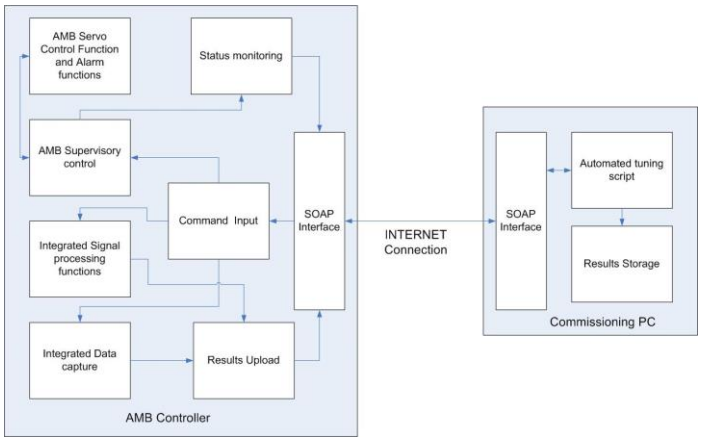

Fig. 6 Automated Commissioning framework.

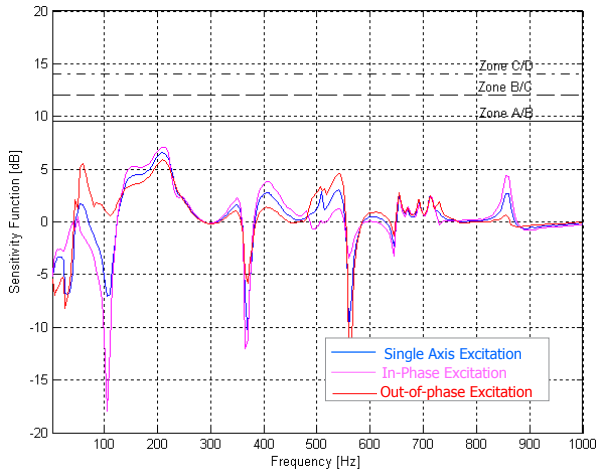

Fig. 7 Sensitivity transfer function measurement with single axis, in-phase, and out-of-phase excitation at standstill.

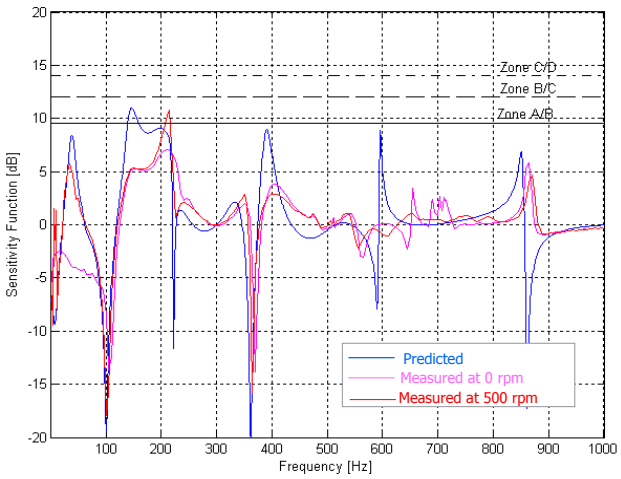

Fig. 8 Sensitivity transfer functions: Predicted, measured at 0 rpm, and measured at 500 rpm.

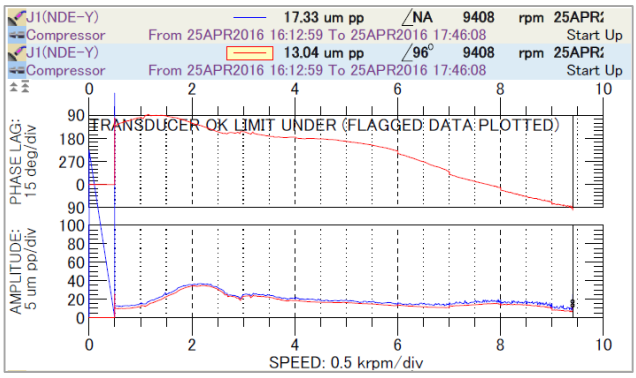

(a) NDE vibration Bode plot

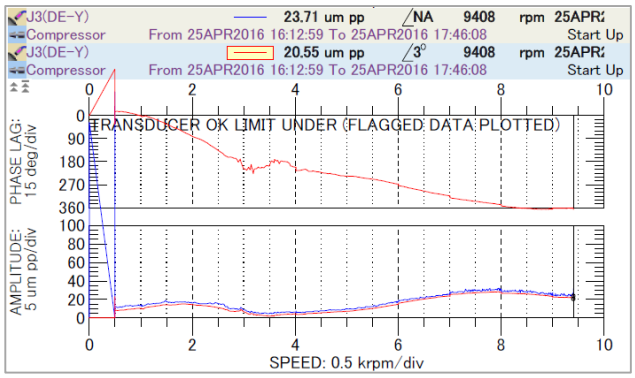

(b) DE vibration Bode plot

Fig. 9 Vibration Bode plots for NDE and DE during mechanical running test.

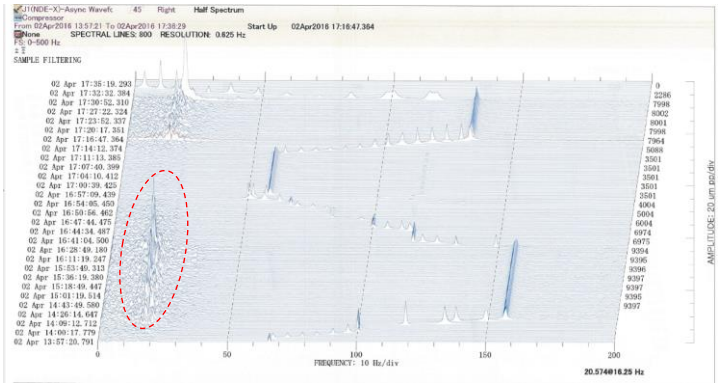

(a) NDE Waterfall Plot

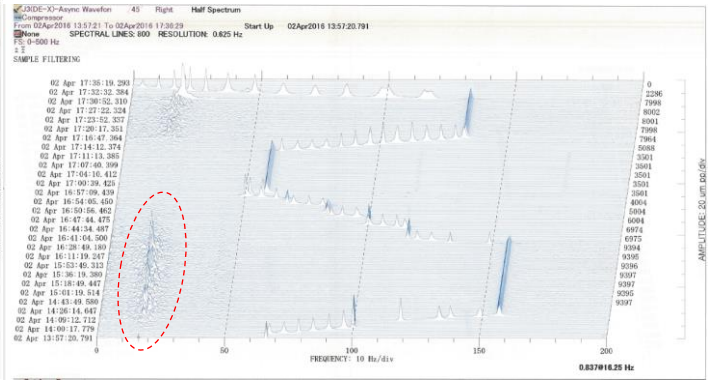

(b) DE Waterfall plot

Fig. 10 Low frequency (20 Hz) response at compressor NDE and DE when the machine was running with 8.9 bar inlet pressure and 17 bar discharge pressure prior to controller optimization.

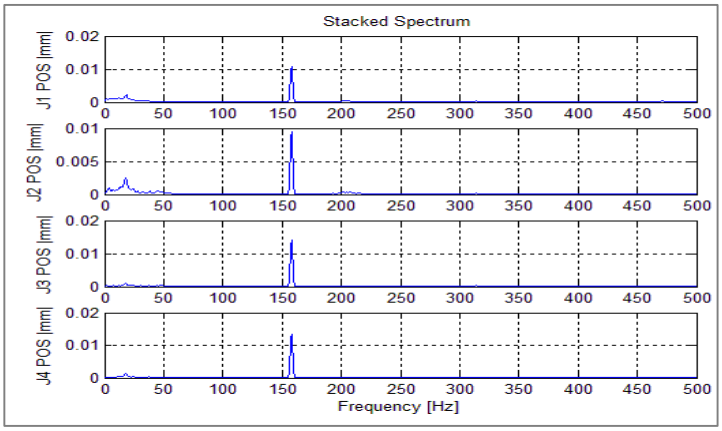

Fig. 11 Vibration spectra with compressor operating at 22 bar-a suction pressure and 63.5 bar-a discharge pressure after optimisation. The plot shows a substantial decrease in subsynchronous activity compared to Fig. 10.